Brain Tumor Pathology (2023) 40:133–141
https://doi.org/10.1007/s10014-023-00451-y

CASE REPORT

High-grade neuroepithelial tumor with *EP300::BCOR* fusion and negative BCOR immunohistochemical expression: a case report

Hirokazu Sugino[1] · Kaishi Satomi[1,2] · Taisuke Mori[1] · Yuuki Mukai[3] · Mai Honda-Kitahara[3] · Yuko Matsushita[4] · Koichi Ichimura[4] · Yoshitaka Narita[3,5] · Akihiko Yoshida[1,5]

Received: 20 November 2022 / Accepted: 5 February 2023 / Published online: 22 February 2023

Abstract

In the World Health Organization tumor classification (fifth edition), central nervous system (CNS) tumors with *BCOR* internal tandem duplications have been recognized as a new tumor type. Some recent studies have reported CNS tumors with *EP300::BCOR* fusions, predominantly in children and young adults, expanding the spectrum of *BCOR*-altered CNS tumors. This study reports a new case of high-grade neuroepithelial tumor (HGNET) with an *EP300::BCOR* fusion in the occipital lobe of a 32-year-old female. The tumor displayed anaplastic ependymoma-like morphologies characterized by a relatively well-circumscribed solid growth with perivascular pseudorosettes and branching capillaries. Immunohistochemically, OLIG2 was focally positive and BCOR was negative. RNA sequencing revealed an *EP300::BCOR* fusion. The Deutsches Krebsforschungszentrum DNA methylation classifier (v12.5) classified the tumor as CNS tumor with *BCOR*/*BCORL1* fusion. The t-distributed stochastic neighbor embedding analysis plotted the tumor close to the HGNET with *BCOR* alteration reference samples. *BCOR*/*BCORL1*-altered tumors should be included in the differential diagnosis of supratentorial CNS tumors with ependymoma-like histological features, especially when they lack *ZFTA* fusion or express OLIG2 even in the absence of BCOR expression. Analysis of published CNS tumors with *BCOR/BCORL1* fusions revealed partly overlapping but not identical phenotypes. Further studies of additional cases are required to establish their classification.

Keywords *BCOR* · *EP300* · Neuroepithelial tumor · Gene fusion

Introduction

BCOR, a member of the polycomb repressive complex that was originally discovered as an interacting corepressor of BCL6, plays a critical role in transcriptional repression [1, 2]. Alterations in *BCOR* have been reported in various tumors of soft tissue, bone, and visceral organs. Pierron et al. were the first to identify bone and soft tissue sarcomas with *BCOR::CCNB3* fusion in adolescents and young adults [3]. Subsequent studies on sarcoma identified broad types of *BCOR* alterations, including *BCOR* fusions with alternative partners [4–6] and internal tandem duplications (ITDs) within exon 15 of *BCOR* [7]. *BCOR* fusion and ITD have also been reported in clear cell sarcoma of the kidney and high-grade endometrial stromal sarcoma [8–12]. Although these tumors with *BCOR* alterations exhibit different clinical characteristics, they are associated with overlapping histological features, including a dense proliferation of uniform oval cells in a variably myxoid and hypervascular stroma, and share

✉ Akihiko Yoshida
akyoshid@ncc.go.jp

1 Department of Diagnostic Pathology, National Cancer Center Hospital, 5-1-1 Tsukiji, Chuo-Ku, Tokyo 104-0045, Japan

2 Department of Pathology, Kyorin University School of Medicine, 6-20-2 Shinkawa, Mitaka, Tokyo 181-8611, Japan

3 Department of Neurosurgery and Neuro-Oncology, National Cancer Center Hospital, 5-1-1 Tsukiji, Chuo-Ku, Tokyo 104-0045, Japan

4 Department of Brain Disease Translational Research, Graduate School of Medicine, Juntendo University, 2-1-1 Hongo, Bunkyo-Ku, Tokyo 113-8421, Japan

5 Rare Cancer Center, National Cancer Center Hospital, 5-1-1 Tsukiji, Chuo-Ku, Tokyo 104-0045, Japan

immunoprofiles, such as overexpression of BCOR and SATB2 [5]. Furthermore, genome-wide DNA methylation analysis identified these tumors as distinct clusters that juxtaposed with one another [13], indicating that they are related but non-identical entities.

In the central nervous system (CNS), *BCOR* ITD was first identified through (epi)genetic analysis of tumors originally diagnosed as primitive neuroectodermal tumors (PNETs) of the CNS [14]. These tumors exhibit characteristic histological findings and DNA methylation profiles [14]. This has led to the proposal of the tumor entity "high-grade neuroepithelial tumor with *BCOR* alteration (HGNET-BCOR)," which has been recently renamed "CNS tumor with *BCOR* internal tandem duplication" in the fifth edition of the World Health Organization (WHO) tumor classification [15]. The tumor affects pediatric and young adult patients and mainly exhibits a solid growth pattern of spindle to oval cells with perivascular pseudorosettes and branching capillary networks [14, 16–18]. Subsequent studies have further described brain tumors with fusions involving *BCOR* or *BCORL1* (a homolog of *BCOR*), such as *EP300::BCORL1* [19], *CREBBP::BCORL1* [20], and *EP300::BCOR* fusions [21–23], which has further expanded the disease concept of *BCOR*-altered brain tumors. However, the clinicopathological and DNA methylation profiles reported for these tumors were not identical [21–23], and whether CNS tumors with *BCOR/BCORL1* fusion represent a single nosologic entity has been a topic of controversy. This study reported a CNS tumor with *EP300::BCOR* fusion and compared its clinicopathological and molecular characteristics with those of previously reported tumors.

Clinical summary

A 32-year-old woman presented to an outside institution with complaints of right-sided visual impairment. The patient was healthy, except for the occurrence of occasional right-sided scintillating scotoma in the past year. The patient was referred to the National Cancer Center Hospital where the visual acuity test revealed right-lower homonymous hemianopsia. Imaging studies revealed a 60-mm mass in the left occipital lobe. The mass was well-circumscribed and hyper-intense on the T2-weighted magnetic resonance (MR) image and hypo-intense to focally hyper-intense on the T1-weighted MR image with heterogeneous gadolinium enhancement (Fig. 1A–D). Calcification and intratumoral hemorrhage were observed. The patient underwent tumor excision, followed by postoperative local radiation (54 Gy) therapy, based on the suspected diagnosis of anaplastic ependymoma. However, the tumor recurred locally 18 months later and was resected. The patient was disease-free three months after the second surgery although the right-lower homonymous hemianopsia was not resolved.

Histopathological and genetic findings

The analysis of the specimen obtained at the first surgery revealed solid growth of uniform small oval cells with prominent perivascular pseudorosettes and branching capillary blood vessels (Fig. 2A–D). The tumor was well-circumscribed. The tumor cells had poorly defined fibrillary cytoplasm and round-to-oval nuclei with fine or granular chromatin and small or inconspicuous nucleoli. The mitotic activity was counted 10 in 2 mm^2. Necrosis, calcification, and focal microvascular proliferation were also observed.

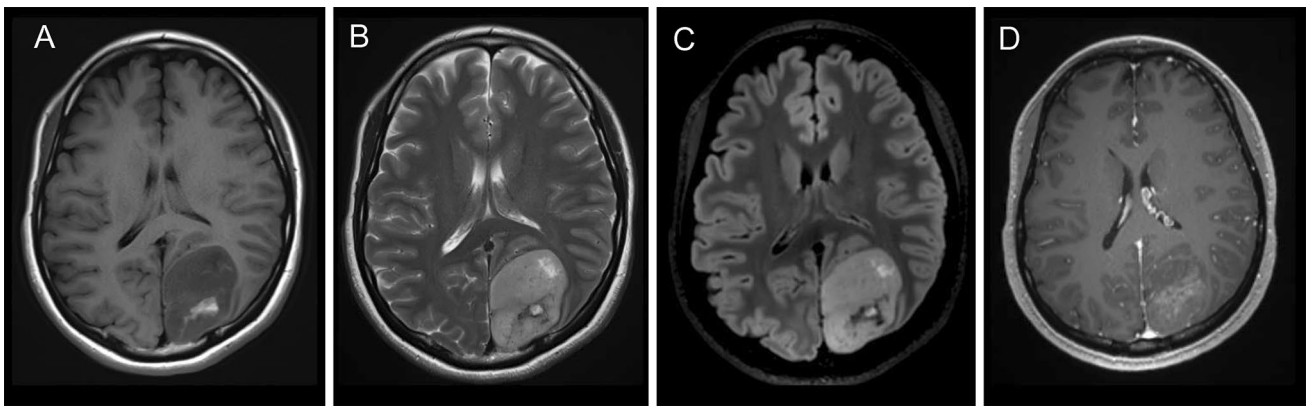

Fig. 1 Magnetic resonance images of a high-grade neuroepithelial tumor with *EP300::BCOR* fusion. **A–D** The magnetic resonance image findings of a primary preoperative tumor. A well-demarcated occipital mass exhibited a hypo-intense signal with a focally hyper-intense signal on a T1-weighted image (**A**) and a hyper-intense signal on a T2-weighted (**B**) and fluid attenuated inversion recovery (FLAIR) (**C**) images. The tumor exhibited heterogeneous enhancement on a gadolinium-enhanced T1-weighted image (**D**)

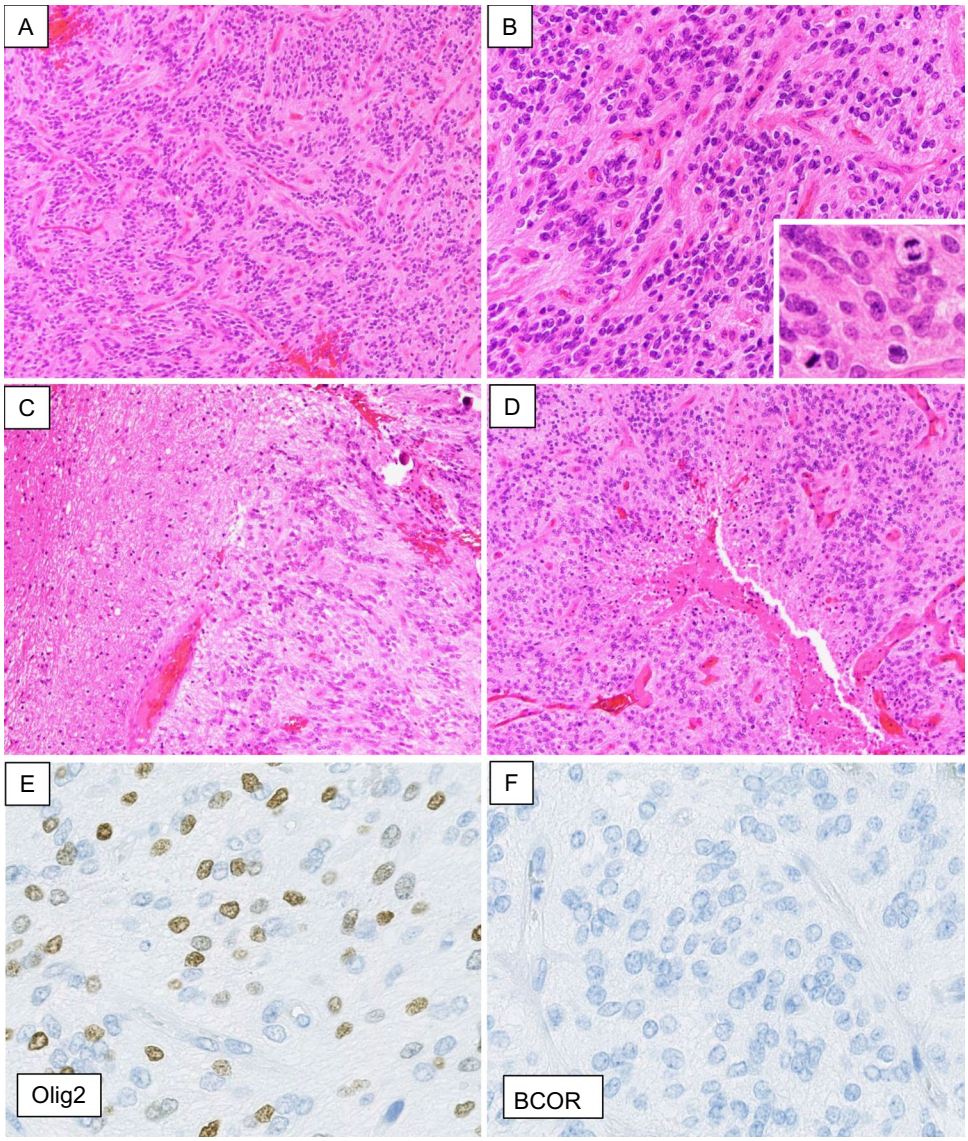

Fig. 2 Histological findings of a high-grade neuroepithelial tumor with *EP300::BCOR* fusion. The tumor comprised uniform small oval cells with prominent perivascular pseudorosettes (**A**, **B**). Mitoses were frequently observed (**B**, inset). The tumor margins were well-demarcated (**C**). Necrosis was observed (**D**). Immunohistochemically, the tumor cells were positive for OLIG2 (**E**) but negative for BCOR (**F**). Original magnification: × 100 (**A**, **C**, **D**), × 200 (**B**), or × 400 (**B** inset, **E**, **F**)

Microcystic changes, Rosenthal fibers, and eosinophilic granular bodies were absent. Immunohistochemical analysis revealed that the tumor tested positive for GFAP, D2-40, and CD99, and focally for OLIG2 (Fig. 2E) but tested negative for IDH1-R132H, epithelial membrane antigen (EMA), BCOR (Fig. 2F), and p65. The Ki-67 labeling index was 40%. The primary antibodies used in the immunohistochemical analysis are listed in Supplementary Table 1.

DNA pyrosequencing, which was performed at the time of diagnosis using methods described previously [19], did not reveal mutations in the *IDH1*, *IDH2*, *H3-3A*, *BRAF*, and *TERT* promoters. Reverse transcription polymerase chain reaction analysis did not reveal *ZFTA::RELA* fusion. The overall histology strongly suggested the diagnosis of anaplastic ependymoma. However, the tumor exhibited unusual features, including focal OLIG2 expression, a lack of *RELA* fusion, and negative p65 expression. Therefore, the definitive diagnosis was deferred, and the case was diagnosed as "glioma, most consistent with anaplastic ependymoma" with a note on the unusual features.

The histological characteristics of the specimen obtained at the second surgery were similar to those of the specimen obtained at the first surgery, including a dense proliferation of uniform oval cells and abundant perivascular pseudorosettes. However, examination of the tumor periphery revealed infiltrating growth of tumor cells that entrapped neurons and neurofilament-positive axons. Immunohistochemical analysis revealed that the tumor tested positive for GFAP, NeuN, and SATB2, and focally for OLIG2 expression. ATRX staining was retained. The tumor was negative for CD34, EMA, synaptophysin, MDM2, and BCOR. This specimen was obtained after the publication by Tauziède-Espariat et al. [22], and we found the tumor shared with their cases some histological features (e.g., perivascular pseudorosettes and

delicate branching capillaries) and BCOR-negative phenotype. Suspecting the presence of *EP300::BCOR* fusion, we performed *BCOR* break-apart fluorescence in situ hybridization (FISH) assay (RP11-77G22 + RP11-665O2 labeled in orange; RP11-91I16 + RP11-1082P20 labeled in green, Chromosome Science Labo, Hokkaido, Japan), which revealed *BCOR* rearrangement in most tumor cells (Fig. 3A). To further characterize *BCOR* fusion, total RNA was extracted from formalin-fixed paraffin-embedded tumor sections. An RNA sequencing library was prepared using a TruSight RNA Pan-Cancer library kit (Illumina, San Diego, CA, USA). The library was subjected to paired-end sequencing on a MiSeq DNA sequencer. The fusion of *EP300* (exon 31, NM_001429.4) and *BCOR* (exon 6, NM_001123385) was identified using the RNA-Seq alignment application (Illumina) (Fig. 3B). Clinical FoundationOne CDx (Foundation Medicine, Cambridge, MA, USA) confirmed the *EP300::BCOR* fusion but no other alterations were detected in the target genes. DNA methylation analysis was performed using an Infinium Methylation EPIC array platform (Illumina). The Deutsches Krebsforschungszentrum (DKFZ) classifier (v11b4) predicted the case as "methylation class CNS high-grade neuroepithelial tumor with *BCOR* alteration" with a low calibrated score of 0.38. However, the newer version of the DKFZ classifier (v12.5) classified the case as "methylation class CNS tumor with *BCOR*/*BCORL1* fusion" with a calibrated score of > 0.99. To perform unsupervised nonlinear dimension reduction, the 1000 most variable probes were selected from the reference samples of 2801 CNS tumors (GSE109381) [24] based on the standard deviation. t-distributed stochastic neighbor embedding (t-SNE) plots were constructed using the Rtsne package (version 0.15). In the t-SNE plots, the tumors were clustered near the HGNET-BCOR reference samples (Fig. 3C). A copy number plot derived from methylome data revealed an overall flat profile (Fig. 3D).

The results of the present case are summarized in Table 1 along with data from previously reported CNS tumors with *BCOR*/*BCORL1* fusion.

Discussion

This report describes a new case of CNS neuroepithelial tumor with *EP300::BCOR* fusion. *EP300::BCOR* fusion was initially reported by two groups in five CNS tumors. However, three tumors described by Torre et al. [21] and two tumors reported by Tauziède-Espariat et al. [22] exhibited different clinicopathological characteristics even though the tumors shared the same fusion profile. The tumors reported by Torre et al. [21] occurred in one female and two males aged 10–18 years and involved the basal ganglia/thalamus, frontal lobe, or occipital lobe. The tumor exhibited an infiltrating growth pattern, a myxoid/microcystic background, and prominent chicken-wire vessels but lacked perivascular pseudorosettes. One case exhibited low-grade histological characteristics, while the other two exhibited high-grade histology (i.e., necrosis, microvascular proliferation, and mitotic activity) in addition to low-grade areas. Immunohistochemical analysis revealed BCOR expression in these tumors. The DKFZ methylation classifier (probably v11b4 based on the publication time) could not classify the tumors. In the t-SNE plots, the three cases clustered together but away from CNS HGNET-BCOR [21]. In contrast, Tauziède-Espariat et al. [22] reported two tumors in the temporal or frontal cerebral lobe involving a 13-year-old man and a 27-year-old man. The tumor formed well-circumscribed masses with minimal peripheral infiltration. Perivascular pseudorosettes, microcyst formation, and chicken-wire vessels were also observed. The tumor exhibited high-grade histological features, such as necrosis, microvascular proliferation, and mitotic activity. The tumors were immunohistochemically negative for BCOR [22]. The DKFZ methylation classifier (probably v11b4 based on the publication time) classified the tumors as HGNET-BCOR [22]. The present tumor resembles the cases reported by Tauziède-Espariat et al. [22] as it exhibited overall circumscription, high-grade histological features, perivascular pseudorosettes, chicken-wire vessels, and BCOR-negative immunophenotype although microcysts were absent. The DKFZ classifier (v11b4) predicted a low-confidence match with HGNET-BCOR. In the t-SNE plot, the tumor was clustered near HGNET-BCOR. Whether these two groups represent separate entities or form the phenotypic spectrum of a single disease is unknown.

The present tumor may also be related to CNS tumors with a fusion involving *BCORL1* (a *BCOR* homolog). Two CNS tumors have been reported to harbor *BCORL1* fusion with related partners. Fukuoka et al. [19] reported a tumor harboring *EP300::BCORL1* fusion in the occipital lobe of a male patient aged 72 years. Similar to the tumor described in this study, the tumor exhibited histological features of anaplastic ependymoma and was classified as HGNET-BCOR by the DKFZ methylation classifier (v11b4) with a low calibrated score of 0.44. Yamazaki et al. [20] described a glioma with *CREBBP::BCORL1* fusion (*CREBBP* is an *EP300* paralog) that exhibited infiltrating growth, microcysts, and a lack of perivascular pseudorosette [20]. The DKFZ classifier (v11b4) could not classify the tumor (score < 0.3). Similar to the present tumor, both cases were classified as "methylation class CNS tumor with *BCOR*/*BCORL1* fusion" by a new version of the classifier (v12.5) [20]. Nonetheless, BCOR expression was positive in the tumor with *CREBBP::BCORL1* and was not reported in the tumor with *EP300::BCORL1*. The role and utility of BCOR expression in tumor classification must be determined in future studies.

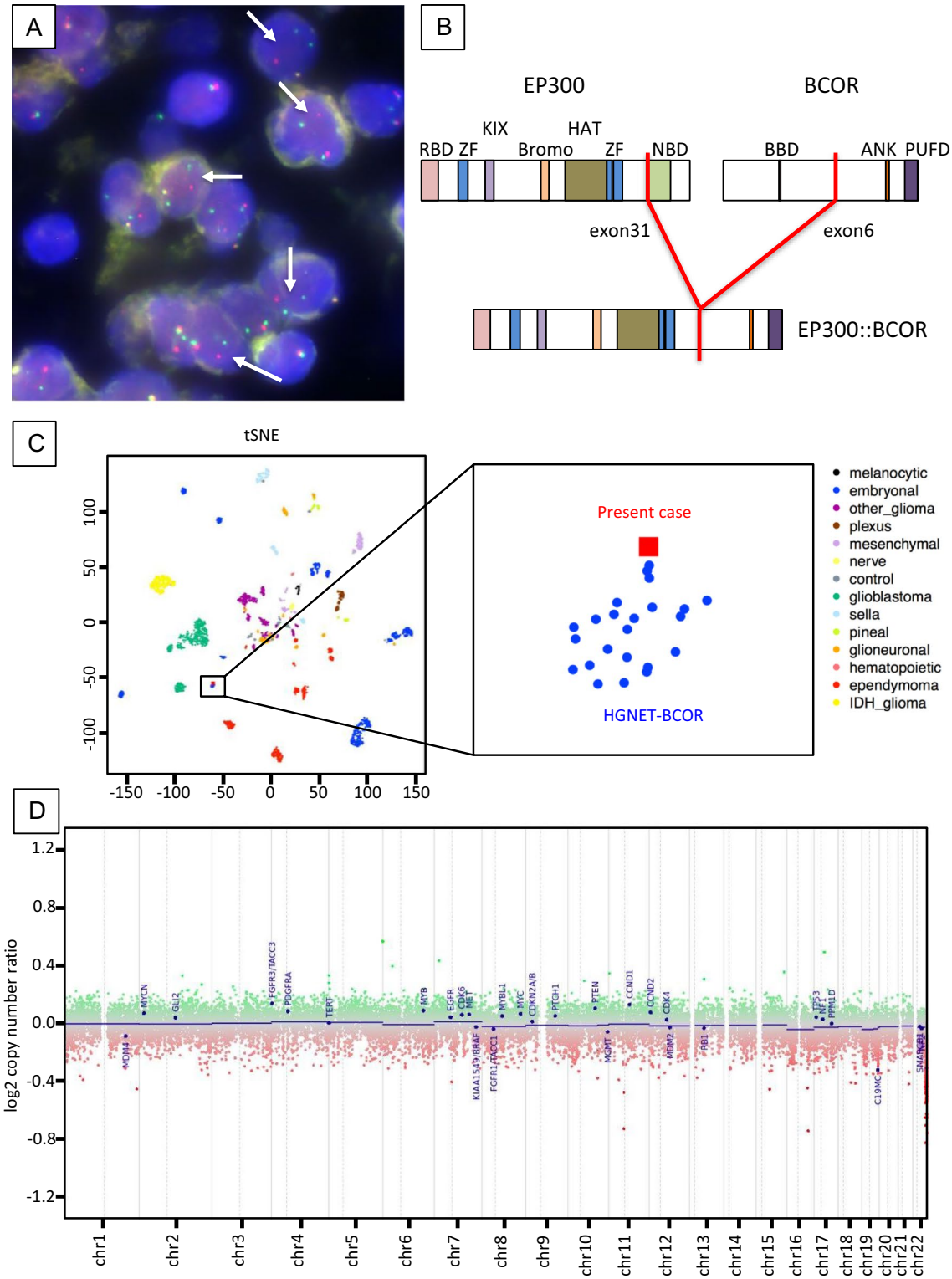

Fig. 3 Molecular findings of a high-grade neuroepithelial tumor with *EP300::BCOR* fusion. **A** *BCOR* break-apart fluorescent in situ hybridization (FISH) analysis. Split green and orange signals (arrows) were observed in most tumor cells, indicating *BCOR* rearrangement. Additional isolated green signals were also observed. **B** Schematic presentation of the predicted chimeric EP300::BCOR protein. RBD, RORA-binding domain; ZF, zinc finger domain; KIX, kinase-inducible domain of CREB-interacting domain; Bromo, bromodomain; HAT, histone acetyltransferase domain; NBD, NCOA2-binding domain; BBD, BCL6-binding domain; ANK, ankyrin repeats; PUFD, PCGF Ub-like fold discriminator. **C** t-distributed stochastic neighbor embedding analysis of DNA methylation data. The present tumor (red square) was clustered near the high-grade neuroepithelial tumor with *BCOR* alteration reference samples (blue dots). **D** Copy number profiling using DNA methylation data demonstrated a relatively silent chromosomal copy number status

Table 1 Reported CNS tumors with *BCOR/BCORL1* fusions

Authors	Age (y)/Sex	Site	Histology						Fusion gene	Methylation class v11b4 or v11b6/ v12.5 or v12b6	Treatment[e]	Recurrence or progression	Outcome (m)
			Growth pattern	Perivascular pseudorosette	Microcyst	Necrosis/ MVP	BCOR IHC	Mitoses					
Present case	32/F	Occipital	Solid[a]	+	–	+/+	–	10, 3/10 HPFs[b]	*EP300*(e31)*::BCOR*(e6)	HGNET-BCOR/MCCNS tumor with BCOR/BCORL1 fusion	R, RT	+	NED (21)
Torre et al. [21]	12/M	Frontal	Invasive	–	+	+/+	+	8/10 HPFs	*EP300*(e31)*::BCOR*(e2)	no match[d]/NA	R	+	AWD (6)
Torre et al. [21]	10/F	Basal ganglia/ thalamus	Invasive	–	+	+/+	+	2, 5/10 HPFs[b]	*EP300*(e31)*::BCOR*(e7)	no match[d]/NA	R, RT	+	NED (7)
Torre et al. [21]	18/M	Occipital	Invasive	–	+	–/–	+	4, 1/10 HPFs[b]	*EP300*(e31)*::BCOR*(e2)	no match[d]/NA	R	+	NED (40)
Tauziède-Espariat et al. [22]	13/M	Temporal	Solid[a]	+	+	+/+	–	High[c]	*EP300*(e31)*::BCOR*(e4)	HGNET-BCOR[d]/NA	R, C	–	NED (16)
Tauziède-Espariat et al. [22]	27/M	Frontal	Solid[a]	+	+	+/+	–	High[c]	*EP300*(e31)::BCOR(e4)	HGNET-BCOR[d]/NA	R, C, RT	–	NED (27)
Wu et al. [23]	5–72/ M:F = 6:5	Frontal, temporal, parietal, occipital, parieto-occipital, temporo-parietal, or posterior fossa	Solid: 2 cases indeterminate: 8 cases NA: 1 case	+: 5 cases –: 5 cases NA: 1 case	NA	+: 7 cases –: 3 cases NA: 1 case/+: 1 case –: 9 cases NA: 1 case	+: 4 cases –: 4 cases NA: 3 cases	Low[c]: 1 case High[c]: 9 cases NA: 1 case	*EP300*(e31)*::BCOR*(e4, e5, e6, or e7)	"MTGF_GBM," HGNET, BCOR, or no match/ CNS tumor with EP300:BCOR(L1) fusion, HGNET with MN1:CXXC5 fusion, neuroepithelial tumor with BCOR ITD, or no match	NA	+: 5 cases –: 4 cases NA: 2 cases	PFS (0.8–86.2)

Table 1 (continued)

Authors	Age (y)/Sex	Site	Histology						Fusion gene	Methylation class v11b4 or v11b6/ v12.5 or v12b6	Treatment[e]	Recurrence or progression	Outcome (m)
			Growth pattern	Perivascular pseudorosette	Microcyst	Necrosis/ MVP	BCOR IHC	Mitoses					
Wu et al. [23]	17/F	Cerebellum	Solid	–	NA	+/+	–	High[c]	*CREBBP*(e31)*::BCOR*(e6)	HGNET, BCOR/ CNS tumor with EP300:BCOR(L1) fusion	NA	–	PFS (2.8)
Fukuoka et al. [19]	72/M	Occipital	NA	+	NA	NA/NA	NA	NA	EP300(e31)*::BCORL1*(e4)	HGNET-BCOR/MC CNS tumor with BCOR/BCORL1 fusion	R(or biopsy), C, RT	+	AWD (33)
Yamazaki et al. [20]	17/F	Frontal	Invasive	–	+	−/−	+	2, 5, 1, 6 /10 HPFs[b]	*CREBBP*(e31)*::BCORL1*(e6)	No match/MC CNS tumor with BCOR/ BCORL1 fusion	R, C, RT	+	DOD (115)
Pisapia et al. [25]	15/M	Frontal, temporal, and occipital	Invasive	NA	NA	+/NA	–	NA	*BCOR*(e4)*::CREBBP*(e31)*	NA/NA	R, C, RT	+	AWD (27)

y years, *F* female, *M* male, *MVP* microvascular proliferation, *IHC* immunohistochemistry, *HPF* high-power field, *e* exon, *HGNET* high-grade neuroepithelial tumor, *CNS* central nervous system, *ITD* internal tandem duplication, *NA* not available, *R* resection, *RT* radiation therapy, *C* chemotherapy, *m* months, *NED* no evidence of disease, *AWD* alive with disease, *DOD* died of disease, *PFS* progression-free survival

[a]Focal infiltration was present

[b]Mitotic counts in specimens from the first and subsequent surgeries

[c]The definitions for "high" and "low" were not stated in the original papers

[d]The classifier version was probable v11b4 based on publication time

[e]Including treatment provided at recurrence or progression

*Unlike in the other cases, this fusion is out of frame

The correlation between BCOR expression and *BCOR* fusion is complex. Immunohistochemical analysis revealed that the present tumor exhibited a BCOR-negative phenotype despite *BCOR* fusion. This can be attributed to the use of anti-BCOR antibody (clone C-10), which recognize 300 amino acid residues at the N-terminal (exons 1, 2, and 3 and a part of exon 4), and the predicted fusion protein lacking an antibody recognition site with a *BCOR* breakpoint in exon 6. Negative BCOR expression of the tumors reported by Tauziède-Espariat et al. [22] can be explained similarly as the tumors had a *BCOR* breakpoint in exon 4. However, the tumors reported by Torre et al. [21] were immunopositive for BCOR even though the *BCOR* breakpoint was in exon 2 or exon 7, contributing to the loss of some or all of the first 300 amino acid residues of BCOR. Furthermore, a glioma with *CREBBP::BCORL1* exhibited upregulated levels of *BCORL1* and *BCOR* mRNAs and was immunopositive for BCOR even though it lacked *BCOR* genetic aberrations [20]. Similar inconsistent BCOR expression has been reported in high-grade endometrial stromal sarcoma with *ZC3H7B::BCOR* fusion [12]. In these tumors, BCOR immunoexpression was reported in 3 cases with *BCOR* breakpoints in exon 7 or 14 [12]. The difference in BCOR expression may involve the breakpoint of *BCOR* fusion and the expression of *BCOR* in the other allele on the X chromosome in women.

Pisapia et al. reported a CNS tumor with a reciprocal fusion combination *BCOR::CREBBP* [25]. The phenotypes of this tumor were completely different from those of the tumors discussed above [21, 22]. The tumor initially manifested as a "gliomatosis cerebri" in a 15-year-old boy [25] with a predominantly low-grade diffuse astrocytoma histology with ATRX loss. BCOR expression was absent, and the tumor harbored *TERT* promoter mutation (c.-124C > T) with no mutations in *IDH1/IDH2* and *H3-3A* [25]. The recurrent tumor after chemoradiotherapy progressed to glioblastoma histology [25]. This reciprocal *BCOR::CREBBP* fusion does not share most exons with *EP300::BCOR* [21, 22] and was predicted to be an out-of-frame fusion resulting in premature stop codon in CREBBP [25], which along with a *TERT* promoter mutation may have influenced phenotypic differences.

Very recently, Wu et al. [23] reported 21 cases of CNS tumors that formed a coherent DNA methylation group and harbored *EP300::BCOR* fusion ($n = 11$), *CREBBP::BCOR* fusion ($n = 1$), *MEAF6::CXXC5* fusion ($n = 1$), or *BCOR* stop-gain mutations ($n = 2$) or exhibited undetermined *BCOR* status ($n = 6$). These cases exhibited variable histological features but likely encompass the characteristics described in this and previous reports [21, 22]. The tumors with *EP300::BCOR* fusion occurred mainly in children and young adults (six males and five females) with the age of occurrence in the range of 5–72 years (median, 21 years), predominantly involving the cerebral hemisphere [23]. Most tumors were indeterminate for peripheral infiltration. Perivascular pseudorosettes were observed in half of the cases [23]. BCOR immunoexpression were observed in 4 of 8 tested cases, which included one case with *EP300::BCOR* fusion that was predicted not to maintain a BCOR antibody recognition site [23]. Most tumors exhibited high mitotic activity and necrosis [23]. The DKFZ classifier (v12b6) classified most tumors with *EP300::BCOR* fusion as "CNS tumor with EP300:BCOR(L1) fusion," while two cases were classified as "neuroepithelial tumor with BCOR internal tandem duplication." [23] One tumor with *MEAF6::CXXC5* fusion was classified as "CNS tumor with EP300:BCOR(L1) fusion" even though it did not exhibit *BCOR* alterations. The imperfect concordance between methylation class, phenotype, and genetic aberrations suggests a complex (epi)genetic/phenotypic relationship and indicates that *EP300::BCOR* fusion is not the sole determinant of tumor characteristics.

In conclusion, we reported a new case of high-grade CNS tumor with *EP300::BCOR* fusion, which exhibited well-circumscribed ependymoma-like histological features and negative BCOR immunoexpression. *BCOR*/*BCORL1*-altered tumors should be considered in the differential diagnosis of supratentorial CNS tumors with ependymoma-like histological features, especially when they lack *ZFTA* fusion or express OLIG2 even in the absence of BCOR expression. CNS tumors with *BCOR/BCORL1* fusions appear to share partly overlapping, but non-identical phenotypes, and further studies of additional cases are required to establish their classification.

Supplementary Information The online version contains supplementary material available at https://doi.org/10.1007/s10014-023-00451-y.

Acknowledgements The authors acknowledge Eijitsu Ryo, Ph.D., for the technical assistance. This work was partly supported by JSPS KAKENHI (Grant Number JP21K06919, AY) and the Rare Cancer Grant (G007, AY).

Author contributions YMu and YN collected the clinical samples and generated the data. HS, KS, and AY performed histological analyses. TM, KS, MH-K, YMa, and KI generated, analyzed, and interpreted the molecular data. HS and AY prepared the manuscript with contributions from all authors.

Data availability The datasets generated and/or analysed during the current study are available from the corresponding author on reasonable request.

Declarations

Conflict of interest The authors declare no competing interests.

Ethical approval This study was approved by the Institutional Review Board of the National Cancer Center Hospital, Tokyo, Japan (No. 2019-297).

References

1. Huynh KD, Fischle W, Verdin E et al (2000) BCoR, a novel corepressor involved in BCL-6 repression. Genes Dev 14:1810–1823
2. Blackledge NP, Rose NR, Klose RJ (2015) Targeting Polycomb systems to regulate gene expression: modifications to a complex story. Nat Rev Mol Cell Biol 16:643–649
3. Pierron G, Tirode F, Lucchesi C et al (2012) A new subtype of bone sarcoma defined by BCOR-CCNB3 gene fusion. Nat Genet 44:461–466
4. Specht K, Zhang L, Sung YS et al (2016) Novel BCOR-MAML3 and ZC3H7B-BCOR gene fusions in undifferentiated small blue round cell sarcomas. Am J Surg Pathol 40:433–442
5. Kao YC, Owosho AA, Sung YS et al (2018) BCOR-CCNB3 fusion positive sarcomas: a clinicopathologic and molecular analysis of 36 cases with comparison to morphologic spectrum and clinical behavior of other round cell sarcomas. Am J Surg Pathol 42:604–615
6. Yoshida A, Arai Y, Hama N et al (2020) Expanding the clinicopathologic and molecular spectrum of BCOR-associated sarcomas in adults. Histopathology 76:509–520
7. Kao YC, Sung YS, Zhang L et al (2016) Recurrent BCOR internal tandem duplication and YWHAE-NUTM2B fusions in soft tissue undifferentiated round cell sarcoma of infancy: overlapping genetic features with clear cell sarcoma of kidney. Am J Surg Pathol 40:1009–1020
8. Roy A, Kumar V, Zorman B et al (2015) Recurrent internal tandem duplications of BCOR in clear cell sarcoma of the kidney. Nat Commun 6:8891
9. Ueno-Yokohata H, Okita H, Nakasato K et al (2015) Consistent in-frame internal tandem duplications of BCOR characterize clear cell sarcoma of the kidney. Nat Genet 47:861–863
10. Lewis N, Soslow RA, Delair DF et al (2018) ZC3H7B-BCOR high-grade endometrial stromal sarcomas: a report of 17 cases of a newly defined entity. Mod Pathol 31:674–684
11. Marino-Enriquez A, Lauria A, Przybyl J et al (2018) BCOR internal tandem duplication in high-grade uterine sarcomas. Am J Surg Pathol 42:335–341
12. Chiang S, Lee CH, Stewart CJR et al (2017) BCOR is a robust diagnostic immunohistochemical marker of genetically diverse high-grade endometrial stromal sarcoma, including tumors exhibiting variant morphology. Mod Pathol 30:1251–1261
13. Koelsche C, Schrimpf D, Stichel D et al (2021) Sarcoma classification by DNA methylation profiling. Nat Commun 12:498
14. Sturm D, Orr BA, Toprak UH et al (2016) New brain tumor entities emerge from molecular classification of CNS-PNETs. Cell 164:1060–1072
15. WHO Classification of Tumours Editorial Board (2021) WHO Classification of Tumours, Central nervous system tumours, 5th ed. International Agency for Research on Cancer World Health Organization, Lyon
16. Appay R, Macagno N, Padovani L et al (2017) HGNET-BCOR tumors of the cerebellum: clinicopathologic and molecular characterization of 3 cases. Am J Surg Pathol 41:1254–1260
17. Kline CN, Joseph NM, Grenert JP et al (2017) Targeted next-generation sequencing of pediatric neuro-oncology patients improves diagnosis, identifies pathogenic germline mutations, and directs targeted therapy. Neuro Oncol 19:699–709
18. Yoshida Y, Nobusawa S, Nakata S et al (2018) CNS high-grade neuroepithelial tumor with BCOR internal tandem duplication: a comparison with its counterparts in the kidney and soft tissue. Brain Pathol 28:710–720
19. Fukuoka K, Kanemura Y, Shofuda T et al (2018) Significance of molecular classification of ependymomas: C11orf95-RELA fusion-negative supratentorial ependymomas are a heterogeneous group of tumors. Acta Neuropathol Commun 6:134
20. Yamazaki A, Arai Y, Fukuoka K et al (2022) Diffusely infiltrating glioma with CREBBP-BCORL1 fusion showing overexpression of not only BCORL1 but BCOR: a case report. Brain Tumor Pathol 39:171–178
21. Torre M, Meredith DM, Dubuc A et al (2019) Recurrent EP300-BCOR fusions in pediatric gliomas with distinct clinicopathologic features. J Neuropathol Exp Neurol 78:305–314
22. Tauziède-Espariat A, Pierron G, Siegfried A et al (2020) The EP300:BCOR fusion extends the genetic alteration spectrum defining the new tumoral entity of "CNS tumors with BCOR internal tandem duplication." Acta Neuropathol Commun 8:178
23. Wu Z, Rajan S, Chung HJ et al (2022) Molecular and clinicopathologic characteristics of gliomas with EP300::BCOR fusions. Acta Neuropathol 144:1175–1178
24. Capper D, Jones DTW, Sill M et al (2018) DNA methylation-based classification of central nervous system tumours. Nature 555:469–474
25. Pisapia DJ, Ohara K, Bareja R et al (2020) Fusions involving BCOR and CREBBP are rare events in infiltrating glioma. Acta Neuropathol Commun 8:80